Guar gum solutions for improved delivery of iron particles in porous media (Part 1): Porous medium rheology and guar gum-induced clogging

Guar gum solutions for improved delivery of iron particles in porous media (Part 1): porous medium rheology and guar gum-induced clogging

Published in

Journal of Contaminant Hydrology

166 (2014) 23–33

Francesca Gastone[(1)], Tiziana Tosco[(1)], Rajandrea Sethi[(1)]*

[(1)] DIATI – Dipartimento di Ingegneria dell'Ambiente, del Territorio e delle Infrastrutture – Politecnico di Torino, C.so Duca degli Abruzzi 24, 10129 Torino, Italy

* Corresponding Author: phone +39 (011) 564 7735; e-mail: rajandrea.sethi@polito.it

Abstract:

The present work is the first part of a comprehensive study on the use of guar gum to improve delivery of microscale zero-valent iron particles in contaminated aquifers. Guar gum solutions exhibit peculiar shear thinning properties, with high viscosity in static conditions and lower viscosity in dynamic conditions: this is beneficial both for the storage of MZVI dispersions, and also for the injection in porous media. In the present paper, the processes associated to guar gum injection in porous media are studied performing single-step and multi-step filtration tests in sand-packed columns. The experimental results of single-step tests performed injecting guar gum solutions prepared at several concentrations and applying different dissolution procedures evidenced that the presence of residual undissolved polymeric particles in the guar gum solution may have a relevant negative impact on the permeability of the porous medium, resulting in evident clogging. The most effective preparation procedure which minimizes the presence of residual particles is dissolution in warm water (60°C) followed by centrifugation (procedure T60C). The multi-step tests (i.e. injection of guar gum at constant concentration with a step increase of flow velocity), performed at three polymer concentrations (1.5, 3 and 4 g/l) provided information on the rheological properties of guar gum solutions when flowing through a porous medium at variable discharge rates, which mimic the injection in radial geometry. An experimental protocol was defined for the rheological characterization of the fluids in porous media, and empirical relationships were derived for the quantification of rheological properties and clogging with variable injection rate. These relationships will be implemented in the second companion paper (Part II) in a radial transport model for the simulation of large-scale injection of MZVI-guar gum slurries.

Keywords:

Guar gum solutions for MZVI delivery, shear thinning flow in porous media, column filtration tests, porous medium clogging.

Graphical abstract:

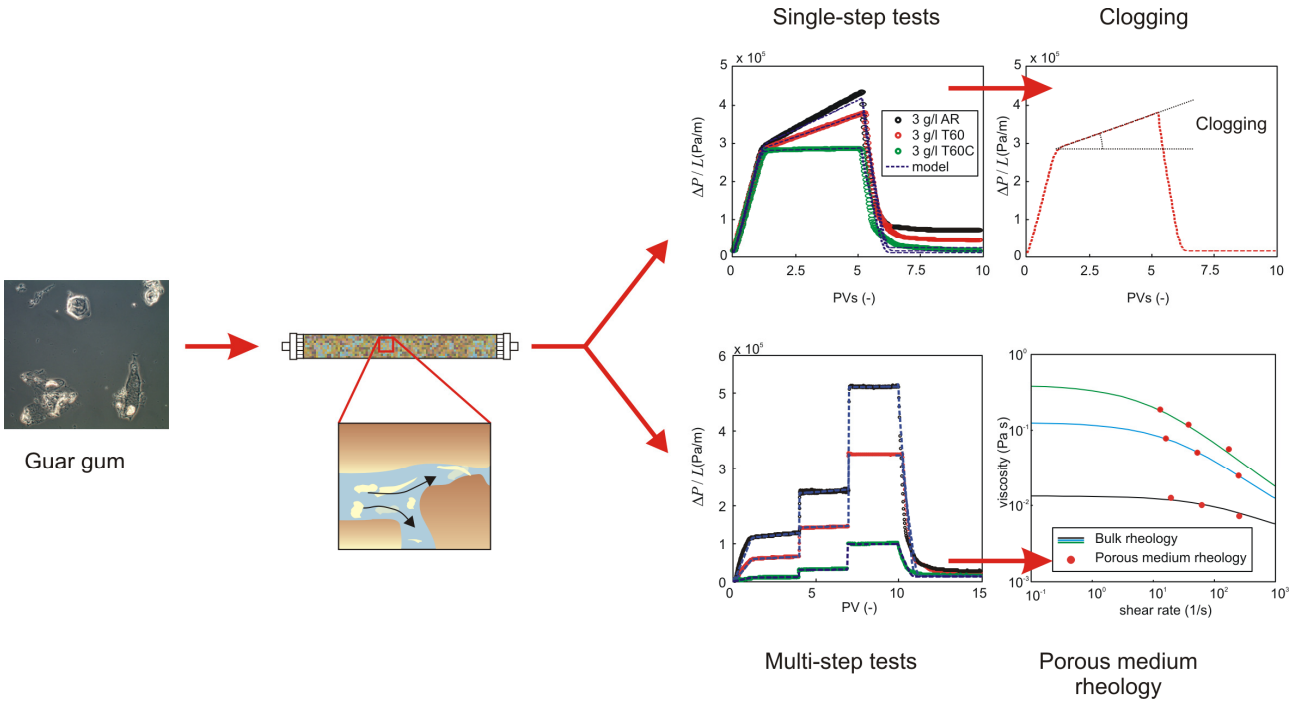

1. Introduction

The injection of water-based slurries of nanoscale and microscale iron particles (NZVI and MZVI) represents a promising in situ remediation technology for contaminated aquifer systems (O'Carroll et al., 2013; Tosco et al., 2014; Yan et al., 2013). Micro and nanoscale iron particles proved effective in reducing a variety of metal ions (DeVor et al., 2006; Jegadeesan et al., 2005; Kanel et al., 2005; Ponder et al., 2000) and degrading a broad range of organic pollutants in groundwater systems, in particular chlorinated hydrocarbons and recalcitrant compounds (Chang et al., 2005; Freyria et al., 2011; He and Zhao, 2005; Joo et al., 2004; Lowry and Johnson, 2004; Zhang, 2003). Since NZVI and MZVI dispersions in pure water are not stable, due to fast aggregation and sedimentation, the use of stabilizers is necessary. Amendments to the particle surfaces which increase inter-particle repulsion forces are effective for NZVI, which is prone to attractive interactions, mainly magnetic in nature (Dalla Vecchia et al., 2009a; Hosseini and Tosco, 2013; Hydutsky et al., 2007; Kocur et al., 2013; Saleh et al., 2007; Schrick et al., 2004; Tiraferri et al., 2008), while modifications of the dispersant fluid is mainly applied for MZVI, which is subject to fast sedimentation (Cantrell et al., 1997; Dalla Vecchia et al., 2009b; Oostrom et al., 2007; Xue and Sethi, 2012). In particular, the increased viscosity of the dispersant fluid resulted in a significantly improved colloidal stability, when "green" biopolymers, like xanthan gum, starch, guar gum and carboxy-methyl-cellulose, were used (Comba et al., 2011; Kocur et al., 2013; Krol et al., 2013; Xue and Sethi, 2012). These polymers, dispersed in water, form non-Newtonian, shear thinning solutions, characterized by a non constant viscosity: in static conditions the viscosity is higher, which is beneficial for storage of the solutions, and in dynamic conditions it is lower, which helps

limiting the pressure build up during injection in the subsurface (Gastone et al., 2014; Xue and Sethi, 2012).

Iron particles are typically delivered to the contaminated area via gravity in wells and piezometers (Elliott and Zhang, 2001; Elliott and Zhang, 2003), or more often via pressure injection applying direct push techniques (Gavaskar et al., 2005; Mueller et al., 2011; Varadhi, 2005; Velimirovic et al., 2014) or using injection wells (Henn and Waddill, 2006). Pressure injection can be performed applying a high injection pressure, thus resulting in the formation of preferential flow paths and porous medium fracturing, or injecting the slurries at low pressure (permeation injection), generating a fairly homogeneous flow through the soil pores (Christiansen et al., 2010; Suthersan, 1999; Tosco et al., 2014). The fracturing approach is used in low to medium permeability formations and when injecting particles whose dimension is in the order of the pore size. Conversely, permeation delivery is preferred in highly permeable formations and, more in general, when particles are small compared to pore size. The threshold between permeation and fracturing injection is related to the critical pressure, that is, the pore pressure which overcomes the porous medium lithostatic load and thus gives rise to preferential flow paths. If permeation is identified as the target delivery method, it is extremely important to limit the pressure build up as much as possible, in order to prevent the possible formation of undesired preferential flow paths (Tosco et al., 2014).

The present work is the first part of a comprehensive study, composed by two papers, on the use of guar gum solutions as dispersant fluids for MZVI delivery via permeation. Guar gum was selected due to its efficacy in improving the colloidal stability of MZVI particles, its environmental compatibility (it is usually adopted in the food industry as a thickening agent), limited cost, and easy degradation in subsurface conditions, especially in the presence of specific enzymes, which can be used to promote the polymer breakage and degradation (Burke and Khan, 2000; Cheng and

Prud'homme, 2000; Di Molfetta and Sethi, 2006; Gastone et al., 2014; Velimirovic et al., 2012; Zolla et al., 2009). In the present Part I, the processes associated with the injection of guar gum solutions in porous media via permeation, as well as approaches and methods for the quantitative analysis and prediction of such processes, are investigated. In Part II, the injection of guar gum-stabilized MZVI in porous media will be studied, and a model for the simulation of field injection of MZVI slurries will be developed and discussed.

When studying the permeation of guar gum in porous media, it is important predict the pressure build up during injection. However, the application of Darcy's law (Darcy, 1856) to guar gum slurries is not straightforward, since neither fluid viscosity nor permeability are not constant parameters: the viscosity is affected by the flow velocity, due to the shear thinning nature of guar gum solutions, and the presence of residual undissolved polymeric particles results in a progressive decrease in permeability during injection (clogging). In this paper, experimental tests and a modeling approach are presented for the prediction of the pressure build up via a modified Darcy's law, which takes into account variable viscosity and permeability. An experimental approach, based on step injection tests, is proposed for the characterization of the rheological properties of guar gum solutions in porous media. Provided that the rheological behavior of the guar gum solutions in the bulk is known (eg. from classical rheological measurements), applying the method herein presented the viscosity of guar gum solutions in the porous medium can be fully characterized. The reduction in permeability, associated with the presence of undissolved polymeric residuals, is considered as well. It is known that the presence of residual particles can be decreased by selecting a proper dissolution procedure (eg. dissolving guar gum powder at a temperature in the range 40°C-70°C), but cannot be completely avoided (Casas J.A., 2000; Chaudemanche and Budtova, 2008; Chauveteau and Kohler, 1984; Gastone et al., 2014). Their presence was shown irrelevant for the overall colloidal stability of the suspension (Gastone et al., 2014), and it has no negative impact on the injectability of guar gum-based slurries via fracturing. Conversely, when delivering via

permeation is desired, the undissolved guar gum particles can clog the porous medium. Moreover, when guar gum solutions are used as delivery fluids for MZVI injection, clogging due to undissolved guar gum produced similar effects to clogging due to the retention of iron particles and aggregates (which will be investigated in details in Part II), both contributing to the overall reduction in porosity and permeability. The quantification of the maximum acceptable pressure build up is not trivial, since the critical pressure for a given porous medium is related to a number of parameters and conditions, discussion of which is beyond the purpose of this work. A control of the overall pressure build up is therefore necessary to prevent fracturing. To this aim, the retention of guar gum particles is to be limited as much as possible, to prevent excessive pressure build up.

In the present paper, clogging due to injection of guar gum solutions is investigated in laboratory column tests (filtration tests), exploring the influence of the guar gum dissolution procedure, and the operating conditions which can minimize clogging are identified. An approach for the modeling of the process is proposed, based on the software E-MNM1D (Tosco and Sethi, 2010), previously developed by the authors. The model is validated against the experimental data of column filtration tests, and simple empirical relationships linking permeability reduction, polymer concentration and injection rate are derived, which will be used in Part II in the MZVI transport model.

2. Background

2.1. Guar gum flow in porous media

The flow of polymeric shear thinning fluids in porous media has been investigated mainly for applications in oil engineering, where these fluids are used in enhanced oil recovery techniques (Muskat and Wyckoff, 1937; Zeinijahromi et al., 2012a), and in the food industry (Lee et al., 2006). When a non-Newtonian fluid flows through a granular medium, the Darcy's law can still be applied in the framework of the generalized Newtonian fluid theory (Bird et al., 1977; Bird et al., 2002): the non-Newtonian flow is represented applying the same laws valid for a Newtonian fluid, provided that the constant Newtonian viscosity is replaced by a shear-dependent viscosity, which takes into account both the rheological properties of the fluid in the bulk, and the additional influence of solid-liquid interface forces (Bird et al., 1977; Lopez et al., 2003; Pearson and Tardy, 2002; Sorbie, 1991; Sorbie et al., 1989). Consequently, in 1-D geometry the Darcy's law for laminar steady state flow becomes

$$-\frac{\Delta p}{L} = \frac{\mu_m(\dot{\gamma}_m)}{K} q \qquad (1)$$

where p is the pressure [M L^{-1} T^{-2}], L is the length of the porous medium [L], q is the specific discharge [L T^{-1}], K is the permeability of the porous medium [L^2], and $\mu_m(\dot{\gamma}_m)$ is the "porous medium viscosity" [M L^{-1} T^{-1}] which depends on the shear rate experienced by the fluid in the porous medium, $\dot{\gamma}_m$ [T^{-1}].

The Cross model (Cross, 1965) can well represent the dependence of bulk viscosity of guar gum solutions on shear rate, $\mu(\dot{\gamma})$, as discussed by the authors in a previous work (Gastone et al., 2014). For a given fluid, the porous medium viscosity obeys the same rheological model of the fluid in the bulk, $\mu(\dot{\gamma})$, provided that a proper definition of shear rate is adopted (Bird et al., 2002; Taylor and Nasr-El-Din, 1998). Therefore the Cross model can be written as (Pearson and Tardy, 2002; Sorbie et al., 1989; Tosco et al., 2013)

$$\begin{cases} \mu_m(\dot{\gamma}_m) = \mu_\infty + \dfrac{\mu_0 - \mu_\infty}{1 + (\lambda \dot{\gamma}_m)^\chi} \\ \dot{\gamma}_m = \alpha \dfrac{|q|}{\sqrt{K\varepsilon}} \end{cases} \tag{2}$$

where ε is the porosity of the medium [-] and μ_0, μ_∞, λ and χ are the Cross parameters of the rheological model in the bulk. The shear rate in the porous medium $\dot{\gamma}_m$ depends on the Darcyan velocity q referred to a characteristic length of the porous medium, namely $\sqrt{K\varepsilon}$ [L] (Perrin et al., 2006; Sorbie, 1991). The shift factor α [-] represents the shift between rheograms of a fluid in the bulk and in the porous medium. This shift was experimentally observed by several authors, and theoretically justified for specific rheological models (Hayes et al., 1996; Liu and Masliyah, 1999; Lopez et al., 2003; Tosco et al., 2013). The shift factor α depends on both rheological properties of the fluids and micro-scale structure of the porous medium, and is expected to be in the order of 1 for well-sorted rounded grains, and higher for irregularly shaped and poorly sorted media (Lopez et al., 2003; Tosco et al., 2013).

Based on equations (1-2), the prediction of the pressure gradient arising from the injection of a shear thinning fluid in a porous medium requires a complete characterization of the fluid viscosity in dynamic conditions, i.e. of the bulk rheological model of the fluid, along with the porous medium properties (permeability and porosity), and the shift factor α.

2.2. Porous medium clogging

The injection of fluids containing particles in a porous medium often results in partial or total clogging. When the amount of retained particles is relevant, the pore size and permeability are reduced, and the pressure gradient consequently increases. Typical examples include industrial applications in deep bed filtration and waste water treatment (Mauclaire et al., 2004), river bank filtration, mobilization of natural colloids in aquifer systems following variations in the pore water chemistry (Dikinya et al., 2008; Mays and Hunt, 2007), and oil reservoir engineering, where clogging is often associated to the mobilization of fines in the proximity of injection or extraction wells (Bedrikovetsky et al., 2012; Zeinijahromi et al., 2012b). Clogging is also observed in the presence of bacterial communities, and is associated both to retention of suspended bacteria and to their growth within the porous medium in a favorable environment (Brovelli et al., 2009; Thullner et al., 2004). A partial clogging of porous media is also often associated to the injection of MZVI and NZVI suspensions (Hosseini and Tosco, 2013; Saleh et al., 2007; Tosco and Sethi, 2010).

Particle retention in porous media can be attributed to a number of mechanisms, including mechanical filtration, straining, sedimentation, and physico-chemical interactions among particles and solid grains (Bradford et al., 2002; Elimelech, 1992; Elimelech, 1994; Rajagopalan and Tien, 1976; Tosco and Sethi, 2009; Tosco et al., 2009; Tufenkji and Elimelech, 2004; Yao et al., 1971). In the case of guar gum solutions, a partial clogging of the porous medium is expected due to presence of large undissolved particles and microgels, which size is of the same order of magnitude of sand grains (Gastone et al., 2014). Sedimentation is unlikely, due to the reduced density contrast between residual particles and pore fluid. Conversely, the retention of particles and poorly hydrated aggregates can be attributed to mechanical filtration and/or straining, and takes place in small and

dead-end pores, thus resulting in a progressive reduction of porosity and permeability (Chauveteau and Kohler, 1984). While particle retention associated to physical-chemical interactions among particles and porous medium can be reversible, particles entrapped in the porous medium due to mechanical filtration are likely to be irreversibly retained (Berthet et al., 2013; Wexler et al., 2013).

A number of modeling approaches are available in the literature for the description of clogging following particles filtration, namely phenomenological approaches for the prediction of head losses (Mays and Hunt, 2005), pore scale-based models (Chen et al., 2009), and macroscopic approaches (Brovelli et al., 2009; Kildsgaard and Engesgaard, 2001). The model herein adopted is based on the macroscopic approach, and links the reduction in permeability to the reduction of porosity and to the formation of irregular deposits within the pores, which increase pore-scale head losses due to friction, and consequently generate additional head losses (Tosco and Sethi, 2010), as discussed in details in paragraph 3.4.

3. Materials and methods

3.1. Materials

Food-grade guar gum (RANTEC HV7000, Ranchester, United States) with nominal maximum particle size of 75 μm was used in the form of dry powder.

Quartz sand (Dorsilit # 8 from Dorfner, Germany) with nominal size 0.3-0.8 mm, measured size distribution $d_{10,sand}$ - $d_{50,sand}$ - $d_{90,sand}$ of 0.22 - 0.28 - 0.33 mm respectively (Static Light Scattering, Beckmann-Coulter LS230, DISAT – Politecnico di Torino) was used in column filtration tests. The sand is mainly composed by quartz (98.9%), with a minor content of K-feldspar as microcline, with measured average grain density of 2.64 g/cm^3. A pre-treatment of the commercial sand with cindering ensures the absence of residual organic matter, thus no specific cleaning procedure was adopted for removing it. Before being used for column packing, the sand was thoroughly rinsed and sonicated to remove any residual colloids and impurities, and finally degassed in a vacuum container to promote the release of residual water bubbles attached to the grain surface. The washing procedure included four cycles of rinsing with deionized water, alternated by sonication cycles of 5 minutes each.

3.2. Guar gum dissolution

Four guar gum dissolution procedures were tested:

- as received (AR): guar gum dissolved in MilliQ water at 20°C with continuous stirring until complete dissolution of the powder (30 min);

- thermally dissolved (T60): the guar gum powder was dissolved in MilliQ water at 60°C, with continuous stirring for 30 min;
- thermally dissolved and wet centrifuged (T60C): the thermally dissolved guar gum (T60) was centrifuged for 10 minutes at a speed of 4000 rpm after the overnight hydration;
- Thermally dissolved and filtered (T60F): the thermally dissolved guar gum (T60) was filtered through a porous medium after the overnight hydration.

For all procedures, immediately after preparation the guar gum solutions were degassed 5 mins using a vacuum pump to remove air bubbles.

Sodium azide was added as a preservative to avoid possible bacterial degradation during storage. Rheological measurements as well as sedimentation and column tests indicated no significant impact of sodium azide on hydration and rheology of the guar gum solutions. Further details on the dissolution procedures are reported in a previous work (Gastone et al., 2014).

The guar gum solutions were prepared at nominal concentrations c_{GG} of 1.5, 3 and 4 g/l. It was observed that, for a given guar gum dissolution procedure, the concentration of residual undissolved particles c_p is directly proportional to the nominal concentration of the solution:

$$c_p = F c_{GG} \tag{3}$$

being F ($0 \leq F \leq 1$) constant for a given preparation procedure. F = 0.12 was assumed for tests of dissolution at room temperature (Ma and Pawlik, 2007), while for T60 and T60C it was determined from column test results.

The rheological characterization of the guar gum solution employed in this paper is reported in a previous work (Gastone et al., 2014), which the reader can refer to for a detailed discussion. Here

only the experimental curves of bulk viscosity versus shear rate, required for the comparison with viscosity values in the porous medium, are reported.

3.3. Column filtration tests

Single-step and multi-step filtration tests were performed injecting guar gum solutions in sand-packed saturated columns. The column was obtained from Plexiglas cylinders (inner diameter 24 mm, outer diameter 32 mm) with Plexiglas pre-filters and screwed/sealed caps at both ends, specifically designed for high pressure injection. The column was wet-packed with the clean sand up to a length of 0.425 m, average porosity ε_0 = 0.37, bulk density $\rho_b = 1.66 \cdot 10^3$ kg/m^3, specific surface area of the porous medium $a_0 = 1.42 \cdot 10^4$ m^2/m^3, permeability $K_0 = 1.56 \pm 0.16 \cdot 10^{-10}$ m^2. The longitudinal dispersivity was assumed equal to the average grain size, $d_{50,sand}$, following the approximation proposed for laboratory-scale transport phenomena (Bear, 1988), and therefore the hydrodynamic dispersion coefficient D_x in the model equations was calculated as $d_{50,sand} \cdot v_e$.

Two progressive cavity pumps (MD 0005-24, Seepex, Germany) were used for the pre-conditioning and flushing with water, and for guar gum injection, respectively (Figure 1). Progressive cavity pumps were preferred as they provide constant flow velocity with no pressure pulses. The discharge rate was periodically monitored during the test, and variations were always below 1%.

Single-step tests were run at constant flow rate (Darcyan velocity $q = 1.88 \pm 0.11 \cdot 10^{-3}$ m/s), to evaluate the impact of the different guar gum dissolution procedures (AR, T60, T60C) on the porous medium clogging for two guar gum concentrations, namely 3 and 4 g/l. The experimental protocol included:

- Pre-flushing with D.I. water (5 PVs);

- Injection of guar gum suspension in D.I. water (5 PVs, 15 PVs for one control test);
- Post-flushing with D.I. water (10 PVs).

Further single-step tests were run at lower Darcy velocity, equal to $q = 4.20 \cdot 10^{-4}$ m/s.

Multi-step filtration tests were then run for the rheological characterization of guar gum solutions in the porous medium. Guar gum solutions at polymer concentrations of 1.5, 3 and 4 g/l were prepared following the T60C procedure. The solutions were injected in the sand-packed columns with a step increase of Darcy velocity, as summarized in **Table 1**. The guar gum injection was preceded by a pre-flushing with DI water at the (low) flow rate of the first guar gum step (5 PVs), and followed by a post flushing at the (high) flow rate of the third guar gum step (10 PVs).

During the tests, the total pressure drop along the column was continuously monitored via pressure sensors at column ends (Delta Ohm, Italy). Contrary to usual column transport tests of dissolved species and colloids, the guar gum concentration in liquid and retained phases was not determined in this work, and consequently the guar gum transport processes were inferred from pressure drop data, rather than from concentration measurements.

3.4. Flow and transport simulations

Clogging was modeled as a reduction of porosity and permeability, dependent on the concentration of guar gum solid particles and microgels retained in the porous medium during injection. The transport of the solid particles dispersed in the solution was modeled by the classical advection-dispersion-deposition equation, modified including a sink term for the particle removal due to retention in the porous medium (Tiraferri et al., 2011; Tosco and Sethi, 2010):

$$\frac{\partial}{\partial t}\left(\varepsilon c_p\right) + \rho_b \frac{\partial s_p}{\partial t} + \frac{\partial}{\partial x}\left(q c_p\right) - \frac{\partial}{\partial x}\left(\varepsilon D_x \frac{\partial c_p}{\partial x}\right) = 0 \qquad (4)$$

where c_p is the concentration of undissolved guar gum solid particles in the solution [M L^{-3}], s_P is the concentration of solid particles retained in the porous matrix, expressed as mass of particles per unit mass of porous medium [M M^{-1}], ε is the porosity [-], D_x is the hydrodynamic dispersion coefficient [L^2 T^{-1}], and ρ_b the bulk density of the porous medium [M L^{-3}]. The second term of eq. (4) expresses the removal of solid particles due to filtration. A first-order irreversible decay with removal rate k_{ap} [T^{-1}] was adopted following the theory for fixed bed filtration (Tien, 1989):

$$\rho_b \frac{\partial s_p}{\partial t} = \varepsilon k_{ap} c_p \tag{5}$$

Irreversible attachment was assumed here since the retention of guar gum particles is likely to be due mainly to mechanical filtration.

The impact of particle retention on the hydrodynamic properties of the porous medium is modeled as a progressive reduction of permeability, due to a concurrent reduction in pore space ε and increase in solid-liquid interface area a, both related to the concentration of retained particles s_p (Mays and Hunt, 2005; Tosco and Sethi, 2010). The empirical Kozeny's relationship (Kozeny, 1927) can be adopted for the dependence of permeability on porosity and specific interface area:

$$K(s_p) = \left(\frac{\varepsilon(s_p)}{\varepsilon_0} \right)^3 \left(\frac{a_0}{a(s_p)} \right)^2 K_0 \tag{6}$$

where ε_0 is the clean bed porosity, i.e. when $s_p = 0$ [-], a_0 is the clean bed specific surface area of the porous matrix [L^{-1}], and K_0 is the clean bed permeability [L^2].

The dependence of porosity and surface area on s_p can be described as:

$$\begin{cases} \varepsilon(s_p) = \varepsilon_0 - \dfrac{\rho_b}{\lambda_p \rho_p} s_p \\ a(s_p) = a_0 + a_p \dfrac{\rho_b}{\rho_p} s \end{cases} \tag{7}$$

where ρ_p is the density of the particles [M L^{-3}], [-], λ_p is the degree of packing of the deposits, expressed as volume of particles per unit volume of particle deposits [-], a_p is the specific surface area of the particles contributing to the overall increase of the solid-liquid interface area [L^{-1}] (Mays and Hunt, 2005).

A modified version of E-MNM1D (Tosco and Sethi, 2010) was used for solving the flow and transport equations (eq. 1-7) in one-dimensional geometry for the fitting of the experimental pressure curves. Porous medium properties (a_0, K_0, ε_0 and ρ_b), particle density ρ_p and dispersion coefficient D_x were assumed as known parameters. Conversely, the contribute of the particles to the increase of specific surface area, a_p, and the filtration rate coefficient, k_{ap}, were determined from data fitting. A graphical interface for E-MNM1D is provided by the software MNMs, which is available for download at www.polito.it/groundwater/software.

4. Results and discussion

4.1. Single-step tests: influence of the preparation procedure on porous medium clogging

Figure **2** reports the experimental results of single-step guar gum filtration tests in terms of normalized pressure drop ΔP_n, calculated as pressure gradient referred to Darcyan velocity, $\Delta P/(Lq)$ [M L^{-3} T^{-1}]. ΔP_n increases linearly during the first pore volume, when guar gum progressively saturates the column. After the first PV, ΔP_n is very similar for all tests, and is directly related to the guar gum viscosity, following the modified Darcy's law (eq. 1). Conversely, the slope $\Delta P_n/PV$ after the first pore volume is approximately constant over time, and can provide a qualitative indication of clogging: the higher the slope, the higher the amount of particles retained, and consequently the reduction in permeability. Curves for T60C and T60F preparation procedures coincide, and therefore only the results for T60C preparation are reported here. The test for the 4 g/l solution, preparation procedure T60, was run for a longer period (15 PVs instead of 5 PVs) to verify the long-term behavior, showing that also in the case of prolonged injection the slope of the curve is almost constant for the whole period.

For both concentrations, the maximum clogging (corresponding to the highest slope, and highest content of undissolved particles) corresponded to dissolution in cold water without any further treatment (AR preparation) (**Figure 3**). The use of warm water improved dissolution (T60), reducing the amount of undissolved particles, and consequently of porous medium clogging. However, the most significant reduction in clogging was obtained when centrifuging (T60C) or filtering (T60F) the guar gum solution.

The results of filtration tests indicate that the use of warm water in the preparation of guar gum solutions is required for improving dissolution, with a moderate reduction of clogging. However, if the application envisioned is the injection in porous media without fracturing, this is not sufficient, because T60 solutions still cause a significant clogging of the column. A post-treatment of the guar gum solution is required for further removal of the residual particles and poorly hydrated aggregates of molecules (microgels). In this sense, both centrifugation and filtration (T60C and T60F) are effective, with a significant reduction of porous medium clogging compared to the other preparation procedures. The efficiency of centrifugation and filtration in removing solid particles and microgels is very similar (Figure **2**b).

4.2. Multi-step tests: rheology of guar gum solutions in the porous medium

The experimental results of multi-step filtration tests are reported in Figure **4** in terms of average pressure gradient along the column, $\Delta P/L$, as a function of the number of pore volumes injected.

An increase in flow rate results in a change in shear rate $\dot{\gamma}_m$, which can be calculated applying eq. (2). Also, for each step the porous medium viscosity, $\mu_m(\dot{\gamma}_m)$, changes accordingly, and can be calculated from the measured pressure gradient as:

$$\mu_m = \frac{K}{q}\frac{\Delta P}{L} \tag{8}$$

As a consequence, each step is characterized by a different viscosity and shear rate, and represents a point of the rheogram of the fluid in the porous medium. The shift factor can be determined as the shift in shear rate required to superimpose the point values obtained from step tests to the bulk

rheogram. Bulk rheograms were previously discussed in (Gastone et al., 2014) and the corresponding Cross parameters are reported in Table 2.

The pressure gradient in the first injection step followed the behavior discussed for single-step injections. The point data exhibit a nice agreement with the bulk rheogram (**Figure 5**), suggesting that the shift factor α is close to the unit. This finding implies that, for future injection tests performed in the same porous medium, the rheological characterization in the bulk is sufficient for a correct simulation of pressure drops (Sorbie et al., 1989; Tosco et al., 2013). A shift factor close to 1 is also in agreement with the literature, that suggests low values in the order of few units in the case of well sorted porous media with regular grain shape, like the sand used in these tests.

4.3. Single-step and multi-step tests: numerical modeling and quantification of clogging

The numerical modeling of the experimental data of column filtration tests evidenced that transport and flow phenomena are strictly coupled since the deposition of a certain amount of particles reduces permeability and porosity, with a double impact on pressure gradient: shear rate increases, decreasing the fluid viscosity (eq. 2) and increasing the pressure gradient (eq.1). On the other hand, a decrease in permeability increases the pressure gradient as well (eq. 1). The overall process is controlled by the content of undissolved particles (c_p), and by the retention kinetics, k_{ap} (eq. 5).

First, the experimental results of the injection step in single-step filtration tests were least-squares fitted to the model equations (1-7) to obtain the unknown parameters controlling flow and clogging phenomena. Unknown parameters include the specific surface area of the residual particles and microgels a_p (which plays a role in determining the reduction of permeability consequent to the deposition of a certain amount of particles), the removal rate k_{ap} (which defines how many particles

are retained) and the fraction of undissolved guar gum mass F. Intuition suggests that both a_p and k_{ap} should not depend on the preparation procedure or guar gum concentration, while F should. As a consequence, all single-step tests were fitted simultaneously for the determination of the three parameters, as reported in **Table 3**. The model-fitted curves are reported in **Figure 2** along with the experimental data. The good agreement between experimental and model results indicates that the assumptions made on the independence (for a_p and k_{ap}) or dependence (for F) of the fitted parameters on the preparation procedure and guar gum concentration is correct.

The fitted value of a_p is quite high, coherently with the irregular shape of the guar gum powder, implying that also a limited quantity of particles retained in the porous medium can significantly reduce the permeability coefficient. The content of undissolved particles F is lower for T60 tests compared to AR tests, and significantly lower for T60C tests, in agreement with the conclusions drawn from the qualitative observation of the experimental results.

The possible dependence of clogging on the flow velocity can be inferred from the combined analysis of single-step and multi-step tests. The model eq. (1-7) were fitted to the experimental data of further tests performed injecting guar gum at lower flow velocity, namely a single step test with $q = 4.20 \cdot 10^{-4}$ m/s, and the first step ($q = 1.13 \cdot 10^{-4}$ m/s) of the multi-step tests. The values of F and a_p determined from the fitting of single-step tests were used in this case, and consequently k_{ap} was the only unknown parameter. A value of k_{ap} was determined for each test (**Figure 6**). When k_{ap} from both single- and multi-step tests and different guar gum concentrations is reported against Darcy velocity (Figure **6**), no evident trend is observed.

As a consequence, it is possible to conclude that, during guar gum injection in a water-saturated medium, the retention kinetics k_{ap} is not significantly affected by the injected concentration nor the flow velocity. An average value of $k_{ap} = 6.3 \cdot 10^{-3}$ s^{-1} is found.

4.4. Guar gum flow processes

The observation of experimental and modeled pressure curves in **Figure 2** and **Figure 4** also provides a deeper insight on the processes controlling the subsequent injection of guar gum and water in porous media. The least-squares fitted pressure curves correctly reproduce the guar gum saturation (first pore volume), and the guar gum injection with clogging. On the contrary, the model does not correctly capture the flushing step: the final experimental pressure drop during post-flushing is underestimated by the simulated curve. Also the modeled decrease in pressure drop in the first pore volume of the flushing (PVs 5 to 6) is slower compared to the experimental data. This discrepancy suggests that the model does not correctly capture the displacement of guar gum by water, and overestimates the final porosity available for water flow.

Furthermore, in multi-step tests (Figure **4**) clogging is more pronounced in the first step, when guar gum is injected at the lowest flow velocity, and decreases with increasing flow velocity. In the last step it is almost negligible. The same trend is observed for all injected concentrations. This finding is only apparently in contrast with the results of modeling, discussed in the previous paragraph, which evidenced an independence of the removal kinetics k_{ap} on the flow velocity both in single-step tests and in the first stage of multi-step tests: in this case, guar gum is injected in a water-saturated medium, while in the second and third injection stages of multi-step tests the porous medium is already saturated in guar gum.

The observed discrepancies can be explained referring to miscible displacement processes (Juanes and Lie, 2007; Obernauer et al., 1994; Singh and Azaiez, 2001; Yan et al., 2013). During the first pore volume water is displaced by guar gum, that is, a viscous fluid is displacing a less viscous one. In this case, the displacement is complete, as suggested by experimental and modeling results in both porous media and capillaries (Malta and Castro, 2009). Even if the transient phenomena arising at the displacement front are different and more complex compared to the Newtonian

displacement (Ciriello and Di Federico, 2012; Ciriello and Di Federico, 2013), the approximation of the generalized Newtonian model and single phase displacement is acceptable. Being the model equations (1-7) based on the hypothesis of single phase flow, experimental and simulated pressure curves are coherent, and a kinetic formulation accounting for constant removal rate k_{ap} is acceptable.

On the other hand, the incorrect simulation of the experimental data of **Figure 2** during the post-flushing suggests that in this case the displacement of guar gum is not complete. Experimental evidence of partial displacement of miscible fluids is reported in the literature when a polymeric viscous fluid (here, guar gum) is displaced by a less viscous one (water) (Obernauer et al., 1994; Petitjeans and Maxworthy, 1996). The phenomenon takes place also for moderate viscosity contrasts (Habermann, 1960; Malta and Castro, 2009), and a residual saturation in the viscous fluid can be observed.

In this study, an incomplete displacement of the guar gum solution is expected to occur during the water front progress (Obernauer et al., 1994), while the removal of the residual polymer remained in the porous medium is expected to take place on a longer period due to progressive dissolution. In this case, the single-phase flow hypothesis assumed in eq. (1-7) does not hold. Similarly, a step change in guar gum injection rate may lead to pore-scale flow processes governed by transients in viscosity, and consequently also in this case the hypothesis of single-phase complete displacement may not be assumed. In this sense, the modeled curves are not reported in **Figure 4** for the second and third injection steps.

Confirmation of an incomplete displacement of guar gum by water can also be inferred from the experimental results of single-step tests (**Figure 2**). Darcy's law was applied at the beginning of the test, end of guar gum injection and end of flushing to calculate, respectively, the clean bed permeability K_0, the permeability at the end of the guar gum injection $K_{end,inj}$ and the permeability at

the end of flushing $K_{end,flush}$. It is observed from the calculated permeability values that $K_{end,flush}$ is significantly lower than $K_{end,inj}$ (Table **4**). This finding cannot be attributed to particle retention, but only to flow-related processes, and specifically to an incomplete displacement of guar gum by water.

Even though it was observed in column filtration tests, the incomplete miscible displacement was not included in the modeling approach because the final aim of this work is to investigate the flow and transport processes related to the injection of guar gum slurries in porous media, for the development of a radial model, and the flushing step is not usually envisioned for field applications. However, the experimental evidence of an incomplete displacement of guar gum by water during flushing is clear, and is to be taken into account for full scale applications of MZVI slurries, even if it is not necessary to model it for the prediction of iron mobility.

5. Conclusions

The present first part of the study concerning the use of guar gum solutions for improved delivery of iron microparticles focused on the flow of guar gum solutions in porous media, and associated processes. A key aspect for guar gum injection is the progressive clogging of the porous medium, due to the presence of particulate and poorly hydrated aggregates of polymer. The incomplete hydration of guar gum powders is an intrinsic property of the material, which cannot be completely avoided. However, the use of warm water during dissolution and, at a higher extent, the application of a post-treatment before injection (centrifugation or filtration) can significantly reduce the quantity of undissolved residual material and, consequently, the associated clogging when the solution is injected in a porous medium. From a practical point of view, the centrifugation (preparation procedure T60C) was preferred in the laboratory, for the easier preparation of the suspensions. However, for field applications the centrifugation of large volumes of guar gum solutions is very unlikely, and therefore an in-line filtration system in fixed bed filters can be envisioned, with largely comparable results in terms of associated clogging.

The estimate of the pressure build up during the injection of shear thinning guar gum solutions in porous media can be obtained applying the Darcy's law extended to non-Newtonian fluids. To this purpose, an estimate of the guar gum viscosity in dynamic conditions in the porous medium is necessary. The literature suggests that the viscosity of a fluid in the porous medium is similar to that of the same fluid in the bulk (which can be easily measured in the laboratory), but is shifted in shear rate of a constant value α, called shift factor, which cannot be easily estimated theoretically. An experimental protocol for step injection tests was therefore proposed and applied for the

determination of the shift factor α: multi-step injection tests were run using the guar gum solutions prepared following the optimized procedure, and the shift factor α was determined comparing rheograms (i.e. viscosity as a function of shear rate) in the bulk (fully characterized in classical rheological measurements) and rheograms obtained from step test data.

The guar gum flow and the associated pressure build up was estimated applying and existing software for the solution of one-dimensional flow and transport problems associated to shear thinning slurries of iron particles (E-MNM1D). The software was modified and successfully simulated the experimental data of guar gum injection in single-step and multi-step column filtration tests. The results of the fitting were analyzed to determine the retention kinetics of undissolved guar gum particles (namely, the coefficient k_{ap}) and to evaluate whether it is affected by the flow velocity. This point in particular is extremely important in the perspective of estimating the pressure build up during injection in the field: since in most delivery techniques the injection can be approximated as a radial flow field (as will be discussed in the companion paper Part II), the flow velocity is not constant with increasing distance from the delivery point, and therefore the relationship between clogging parameters and the flow velocity is to be known. The numerical modeling of the experimental results evidenced an independence of k_{ap} on flow velocity, and an average value of the retention kinetics was determined. It will be used for the simulation of additional pressure drop due to guar gum retention during the injection of microscale iron slurries in radial geometry, which is the topic of the second part of this study.

Acknowledgement

The work was co-funded by the EU research project AQUAREHAB (FP7, Grant Agreement n. 226565).

References

Bear, J., 1988. Dynamics of fluids in porous media. Dover books on physics and chemistry. Dover, New York, xvii, 764 p. pp.

Bedrikovetsky, P., Zeinijahromi, A., Siqueira, F.D., Furtado, C.A. and de Souza, A.L.S., 2012. Particle Detachment Under Velocity Alternation During Suspension Transport in Porous Media. Transport in Porous Media, 91(1): 173-197.

Berthet, H., Fermigier, M. and Lindner, A., 2013. Single fiber transport in a confined channel: Microfluidic experiments and numerical study. Physics of Fluids (1994-present), 25(10): -.

Bird, R.B., Armstrong, R.C. and Hassager, O., 1977. Dynamics of polymeric liquids. Volume 1. Fluid mechanics. John Wiley and Sons Inc., New York - NY.

Bird, R.B., Stewart, W.E. and Lightfoot, E.N., 2002. Transport phenomena. J. Wiley, New York, xii, 895 p. pp.

Bradford, S.A., Yates, S.R., Bettahar, M. and Simunek, J., 2002. Physical factors affecting the transport and fate of colloids in saturated porous media. Water Resources Research, 38(12): Doi 10.1029/2002wr001340.

Brovelli, A., Malaguerra, F. and Barry, D.A., 2009. Bioclogging in porous media: Model development and sensitivity to initial conditions. Environmental Modelling & Software, 24(5): 611-626.

Burke, M.D. and Khan, S.A., 2000. Triggered enzymatic degradation of a water-soluble polymer solution using a novel inhibitor. Biomacromolecules, 1(4): 688-695.

Cantrell, K.J., Kaplan, D.I. and Gilmore, T.J., 1997. Injection of colloidal Fe0 particles in sand with shear-thinning fluids. Journal of Environmental Engineering, 123(8): 786-791.

Casas J.A., A.F.M., Ochoa F. G., 2000. Viscosity of guar gum and xanthan/guar gum mixture solutions. Journal of the Science of Food and Agriculture, 80: 1722-1727.

Chang, M.C., Shu, H.Y., Hsieh, W.P. and Wang, M.C., 2005. Using nanoscale zero-valent iron for the remediation of polycyclic aromatic hydrocarbons contaminated soil. Journal of the Air & Waste Management Association, 55(8): 1200-1207.

Chaudemanche, C. and Budtova, T., 2008. Mixtures of pregelatinised maize starch and κ-carrageenan: Compatibility, rheology and gelation. Carbohydrate Polymers, 72(4): 579-589.

Chauveteau, G. and Kohler, N., 1984. Influence of microgels in polysaccharide solutions on their flow behavior through porous media. Society of Petroleum Engineers journal, 24(3): 361-368.

Chen, C., Lau, B.L.T., Gaillard, J.F. and Packman, A.I., 2009. Temporal evolution of pore geometry, fluid flow, and solute transport resulting from colloid deposition. Water Resources Research, 45: Doi 10.1029/2008wr007252.

Cheng, Y. and Prud'homme, R.K., 2000. Enzymatic degradation of guar and substituted guar galactomannans. Biomacromolecules, 1(4): 782-788.

Christiansen, C.M., Damgaard, I., Broholm, M., Kessler, T., Klint, K.E., Nilsson, B. and Bjerg, P.L., 2010. Comparison of delivery methods for enhanced in situ remediation in clay till. Ground Water Monitoring and Remediation, 30(4): 107-122.

Ciriello, V. and Di Federico, V., 2012. Similarity solutions for flow of non-Newtonian fluids in porous media revisited under parameter uncertainty. Advances in Water Resources, 43: 38-51.

Ciriello, V. and Di Federico, V., 2013. Analytical modeling of spherical displacement for power-law fluids in porous media. Applied Mathematical Sciences, 7(57-60): 2993-3005.

Comba, S., Dalmazzo, D., Santagata, E. and Sethi, R., 2011. Rheological characterization of xanthan suspensions of nanoscale iron for injection in porous media. Journal of Hazardous Materials, 185(2–3): 598-605.

Cross, M.M., 1965. Rheology of non-Newtonian fluids: A new flow equation for pseudoplastic systems. Journal of Colloid Science, 20(5): 417-437.

Dalla Vecchia, E., Coisson, M., Appino, C., Vinai, F. and Sethi, R., 2009a. Magnetic Characterization and Interaction Modeling of Zerovalent Iron Nanoparticles for the Remediation of Contaminated Aquifers. Journal of Nanoscience and Nanotechnology, 9(5): 3210-3218.

Dalla Vecchia, E., Luna, M. and Sethi, R., 2009b. Transport in Porous Media of Highly Concentrated Iron Micro- and Nanoparticles in the Presence of Xanthan Gum. Environmental Science & Technology, 43(23): 8942-8947.

Darcy, H., 1856. Les fontaines publiques de la ville de Dijon. Dalmont, Paris.

DeVor, R., Geiger, C.L., Clausen, C.A., Quinn, J. and Milum, K.M., 2006. tEmulsified nanoscale iron particles for environmental remediation of heavy metals. Abstracts of Papers of the American Chemical Society, 231: -.

Di Molfetta, A. and Sethi, R., 2006. Clamshell excavation of a permeable reactive barrier. Environmental Geology.

Dikinya, O., Hinz, C. and Aylmore, G., 2008. Decrease in hydraulic conductivity and particle release associated with self-filtration in saturated soil columns. Geoderma, 146(1-2): 192-200.

Elimelech, M., 1992. Predicting collision efficiencies of colloidal particles in porous media. Water Research, 26(1): 1-8.

Elimelech, M., 1994. Effect of Particle Size on the Kinetics of Particle Deposition under Attractive Double Layer Interactions. Journal of Colloid and Interface Science, 164(1): 190-199.

Elliott, D.W. and Zhang, W.X., 2001. Field assessment of nanoscale bimetallic particles for groundwater treatment. Environmental Science and Technology, 35(24): 4922-4926.

Elliott, D.W. and Zhang, W.X., 2003. Field assessment of nanoscale bimetallic particles for groundwater treatment. Abstracts of Papers of the American Chemical Society, 225: U971-U971.

Freyria, F.S., Bonelli, B., Sethi, R., Armandi, M., Belluso, E. and Garrone, E., 2011. Reactions of Acid Orange 7 with Iron Nanoparticles in Aqueous Solutions. The Journal of Physical Chemistry C, 115(49): 24143-24152.

Gastone, F., Tosco, T. and Sethi, R., 2014. Green stabilization of microscale iron particles using guar gum: bulk rheology, sedimentation rate and enzymatic degradation. Journal of Colloid and Interface Science, 421: 33-43.

Gavaskar, A., L., T. and Condit, W., 2005. Cost And Performance Report Nanoscale Zero-Valent Iron Technologies For Source Remediation.

Habermann, B., 1960. The Efficiency of Miscible Displacement As A Function of Mobility Ratio. Petroleum Transactions, 219: 264-272.

Hayes, R.E., Afacan, A., Boulanger, B. and Shenoy, A.V., 1996. Modelling the flow of power law fluids in a packed bed using a volume-averaged equation of motion. Transport in Porous Media, 23(2): 175-196.

He, F. and Zhao, D.Y., 2005. Preparation and characterization of a new class of starch-stabilized bimetallic nanoparticles for degradation of chlorinated hydrocarbons in water. Environmental Science & Technology, 39(9): 3314-3320.

Henn, K.W. and Waddill, D.W., 2006. Utilization of nanoscale zero-valent iron for source remediation—A case study. Remediation Journal, 16(2): 57-77.

Hosseini, S.M. and Tosco, T., 2013. Transport and retention of high concentrated nano-Fe/Cu particles through highly flow-rated packed sand column. Water Research, 47(1): 326-338.

Hydutsky, B.W., Mack, E.J., Beckerman, B.B., Skluzacek, J.M. and Mallouk, T.E., 2007. Optimization of nano- and microiron transport through sand columns using polyelectrolyte mixtures. Environmental Science & Technology, 41(18).

Jegadeesan, G., Mondal, K. and Lalvani, S.B., 2005. Arsenate remediation using nanosized modified zerovalent iron particles. Environmental Progress, 24(3): 289-296.

Joo, S.H., Feitz, A.J. and Waite, T.D., 2004. Oxidative degradation of the carbothioate herbicide, molinate, using nanoscale zero-valent iron. Environmental Science & Technology, 38(7): 2242-2247.

Juanes, R. and Lie, K.-A., 2007. Numerical modeling of multiphase first-contact miscible flows. Part 1. Analytical Riemann solver. Transport in Porous Media, 67(3): 375-393.

Kanel, S.R., Manning, B., Charlet, L. and Choi, H., 2005. Removal of arsenic(III) from groundwater by nanoscale zero-valent iron. Environmental Science & Technology, 39(5): 1291-1298.

Kildsgaard, J. and Engesgaard, P., 2001. Numerical analysis of biological clogging in two-dimensional sand box experiments. Journal of Contaminant Hydrology, 50(3-4): 261-285.

Kocur, C.M., O'Carroll, D.M. and Sleep, B.E., 2013. Impact of nZVI stability on mobility in porous media. Journal of Contaminant Hydrology, 145: 17-25.

Kozeny, J., 1927. Uber Kapillare Leitung des Wasser im Boden. *Sitzungsberichte der Akademie der Wissenschaften Wien* **136**: 106-271.

Krol, M.M., Oleniuk, A.J., Kocur, C.M., Sleep, B.E., Bennett, P., Zhong, X. and O'Carroll, D.M., 2013. A Field-Validated Model for In Situ Transport of Polymer-Stabilized nZVI and Implications for Subsurface Injection. Environmental Science & Technology.

Lee, S., Ang, W.S. and Elimelech, M., 2006. Fouling of reverse osmosis membranes by hydrophilic organic matter: Implications for water reuse. Desalination, 187(1-3): 313-321.

Liu, S. and Masliyah, J.H., 1999. Non-linear flows in porous media. Journal of Non-Newtonian Fluid Mechanics, 86(1-2): 229-252.

Lopez, X., Valvatne, P.H. and Blunt, M.J., 2003. Predictive network modeling of single-phase non-Newtonian flow in porous media. Journal of Colloid and Interface Science, 264(1): 256-265.

Lowry, G.V. and Johnson, K.M., 2004. Congener specific dechlorination of dissolved PCBs by nanoscale zero-valent iron at ambient pressure and temperature. Abstracts of Papers of the American Chemical Society, 228: U607-U607.

Ma, X. and Pawlik, M., 2007. Role of background ions in guar gum adsorption on oxide minerals and kaolinite. Journal of Colloid and Interface Science, 313(2): 440-448.

Malta, S.M.C. and Castro, R.G.S., 2009. Finite-element simulations of miscible fingering problems. International Journal of Computer Mathematics, 87(9): 2053-2063.

Mauclaire, L., Schurmann, A., Thullner, M., Gammeter, S. and Zeyer, J., 2004. Sand filtration in a water treatment plant: biological parameters responsible for clogging. Journal of Water Supply Research and Technology-Aqua, 53(2): 93-108.

Mays, D.C. and Hunt, J.R., 2005. Hydrodynamic aspects of particle clogging in porous media. Environmental Science & Technology, 39(2): 577-584.

Mays, D.C. and Hunt, J.R., 2007. Hydrodynamic and chemical factors in clogging by montmorillonite in porous media. Environmental Science & Technology, 41(16): 5666-5671.

Mueller, N.C., Braun, J., Bruns, J., Cernik, M., Rissing, P., Rickerby, D. and Nowack, B., 2011. Application of nanoscale zero valent iron (NZVI) for groundwater remediation in Europe. Environmental Science and Pollution Research.

Muskat, M. and Wyckoff, R.D., 1937. The flow of homogeneous fluids through porous media. International series in physics. McGraw-Hill Book Company, inc., New York, London,, xix, 763 p. pp.

O'Carroll, D., Sleep, B., Krol, M., Boparai, H. and Kocur, C., 2013. Nanoscale zero valent iron and bimetallic particles for contaminated site remediation. Advances in Water Resources, 51: 104-122.

Obernauer, S., Temprano, N., Chertcoff, R., D'Onofrio, A.G., Gabbanelli, S. and M., R., 1994. Miscible Displacement of Polymers in Porous Media, SPE Latin America/Caribbean Petroleum Engineering Conference. Society of Petroleum Engineers Inc., Buenos Aires, Argentina.

Oostrom, M., Wietsma, T.W., Covert, M.A. and Vermeul, V.R., 2007. Zero-Valent Iron Emplacement in Permeable Porous Media Using Polymer Additions. Ground Water Monitoring & Remediation, 27(1): 122-130.

Pearson, J.R.A. and Tardy, P.M.J., 2002. Models for flow of non-Newtonian and complex fluids through porous media. Journal of Non-Newtonian Fluid Mechanics, 102(2): 447-473.

Perrin, C.L., Tardy, P.M.J., Sorbie, K.S. and Crawshaw, J.C., 2006. Experimental and modeling study of Newtonian and non-Newtonian fluid flow in pore network micromodels. Journal of Colloid and Interface Science, 295(2): 542-550.

Petitjeans, P. and Maxworthy, T., 1996. Miscible displacements in capillary tubes. Part 1. Experiments. Journal of Fluid Mechanics, 326: 37-56.

Ponder, S.M., Darab, J.G. and Mallouk, T.E., 2000. Remediation of Cr(VI) and Pb(II) aqueous solutions using supported, nanoscale zero-valent iron. Environmental Science & Technology, 34(12): 2564-2569.

Rajagopalan, R. and Tien, C., 1976. Trajectory analysis of deep-bed filtration with the sphere-in-cell porous media model. Aiche Journal, 22(3): 523-533.

Saleh, N., Sirk, K., Liu, Y., Phenrat, T., Dufour, B., Matyjaszewski, K., Tilton, R.D. and Lowry, G.V., 2007. Surface modifications enhance nanoiron transport and NAPL targeting in saturated porous media. Environmental Engineering Science, 24(1): 45-57.

Schrick, B., Hydutsky, B.W., Blough, J.L. and Mallouk, T.E., 2004. Delivery vehicles for zerovalent metal nanoparticles in soil and groundwater. Chemistry of Materials, 16(11): 2187-2193.

Singh, B.K. and Azaiez, J., 2001. Numerical simulation of viscous fingering of shear-thinning fluids. Canadian Journal of Chemical Engineering, 79(6): 961-967.

Sorbie, K.S., 1991. Polymer-improved oil recovery. Blackie ; CRC Press, Glasgow, Boca Raton, Fla., xii, 359 p. pp.

Sorbie, K.S., Clifford, P.J. and Jones, E.R.W., 1989. The rheology of pseaudoplastic fluids in porous media using network modeling. Journal of Colloid and Interface Science, 130(2): 508-534.

Suthersan, S.S., 1999. Hydraulic and Pneumatic Fracturing.

Taylor, K.C. and Nasr-El-Din, H.A., 1998. Water-soluble hydrophobically associating polymers for improved oil recovery: A literature review. Journal of Petroleum Science and Engineering, 19(3-4): 265-280.

Thullner, M., Schroth, M.H., Zeyer, J. and Kinzelbach, W., 2004. Modeling of a microbial growth experiment with bioclogging in a two-dimensional saturated porous media flow field. Journal of Contaminant Hydrology, 70(1-2): 37-62.

Tien, C., 1989. Granular filtration of aerosols and hydrosols. Butterworths series in chemical engineering. Butterworths, Boston, xii, 365 p. pp.

Tiraferri, A., Chen, K.L., Sethi, R. and Elimelech, M., 2008. Reduced aggregation and sedimentation of zero-valent iron nanoparticles in the presence of guar gum. Journal of Colloid and Interface Science, 324(1-2): 71-79.

Tiraferri, A., Tosco, T. and Sethi, R., 2011. Transport and retention of microparticles in packed sand columns at low and intermediate ionic strengths: Experiments and mathematical modeling. Environmental Earth Sciences, 63(4): 847-859.

Tosco, T., Marchisio, D.L., Lince, F. and Sethi, R., 2013. Extension of the Darcy-Forchheimer Law for Shear-Thinning Fluids and Validation via Pore-Scale Flow Simulations. Transport in Porous Media, 96(1): 1-20.

Tosco, T., Petrangeli Papini, M., Cruz Viggi, C. and Sethi, R., 2014. Nanoscale iron particles for groundwater remediation: a review. Journal of Cleaner Production: DOI: 10.1016/j.jclepro.2013.12.026.

Tosco, T. and Sethi, R., 2009. MNM1D: a numerical code for colloid transport in porous media: implementation and validation. American Journal of Environmental Sciences, 5(4): 517-525.

Tosco, T. and Sethi, R., 2010. Transport of non-newtonian suspensions of highly concentrated micro- and nanoscale iron particles in porous media: A modeling approach. Environmental Science and Technology, 44(23): 9062-9068.

Tosco, T., Tiraferri, A. and Sethi, R., 2009. Ionic Strength Dependent Transport of Microparticles in Saturated Porous Media: Modeling Mobilization and Immobilization Phenomena under Transient Chemical Conditions. Environmental Science & Technology, 43(12): 4425-4431.

Tufenkji, N. and Elimelech, M., 2004. Correlation equation for predicting single-collector efficiency in physicochemical filtration in saturated porous media. Environmental Science & Technology, 38(2): 529-536.

Varadhi, S., Harch, G., Apoldo, L., Liao, Blackman, R., Wittman, W. , 2005. Full-scale nanoiron injection for treatment of groundwater contaminated with chlorinated hydrocarbons., *The Natural Gas Technologies 2005 Conference*.

Velimirovic, M., Chen, H., Simons, Q. and Bastiaens, L., 2012. Reactivity recovery of guar gum coupled mZVI by means of enzymatic breakdown and rinsing. Journal of Contaminant Hydrology, 142-143: 1-10.

Velimirovic, M., Tosco, T., Uyttebroek, M., Luna, M., Gastone, F., De Boer, C., Klaas, N., Sapion, H., Eisenmann, H., Larsson, P.-O., Braun, J., Sethi, R. and Bastiaens, L., 2014. Field assessment of guar gum stabilized microscale zerovalent iron particles for in-situ remediation of 1,1,1-trichloroethane. Journal of Contaminant Hydrology, 164(0): 88-99.

Wexler, J.S., Trinh, P.H., Berthet, H., Quennouz, N., Du Roure, O., Huppert, H.E., Linder, A. and Stone, H.A., 2013. Bending of elastic fibres in viscous flows: The influence of confinement. Journal of Fluid Mechanics, 720: 517-544.

Xue, D. and Sethi, R., 2012. Viscoelastic gels of guar and xanthan gum mixtures provide long-term stabilization of iron micro- and nanoparticles. Journal of Nanoparticle Research, 14(11).

Yan, W., Lien, H.-L., Koel, B.E. and Zhang, W.-x., 2013. Iron nanoparticles for environmental clean-up: recent developments and future outlook. Environmental Science: Processes & Impacts, 15(1): 63-77.

Yao, K.-M., Habibian, M.T. and O'Melia, C.R., 1971. Water and waste water filtration. Concepts and applications. Environmental Science & Technology, 5(11): 1105-1112.

Zeinijahromi, A., Vaz, A. and Bedrikovetsky, P., 2012a. Well impairment by fines migration in gas fields. Journal of Petroleum Science and Engineering.

Zeinijahromi, A., Vaz, A. and Bedrikovetsky, P., 2012b. Well impairment by fines migration in gas fields. Journal of Petroleum Science and Engineering, 88-89: 125-135.

Zhang, W.X., 2003. Nanoscale iron particles for environmental remediation: An overview. Journal of Nanoparticle Research, 5(3-4): 323-332.

Zolla, V., Freyria, F.S., Sethi, R. and Di Molfetta, A., 2009. Hydrogeochemical and Biological Processes Affecting the Long-term Performance of an Iron-Based Permeable Reactive Barrier. J. Environ. Qual., 38(3): 897-908.

Figure captions

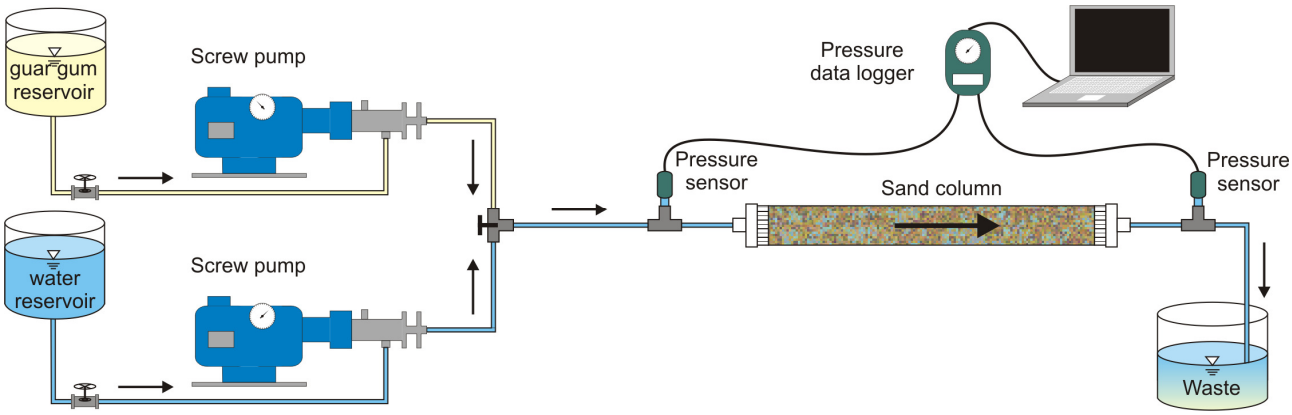

Figure 1: Experimental setup for column filtration tests

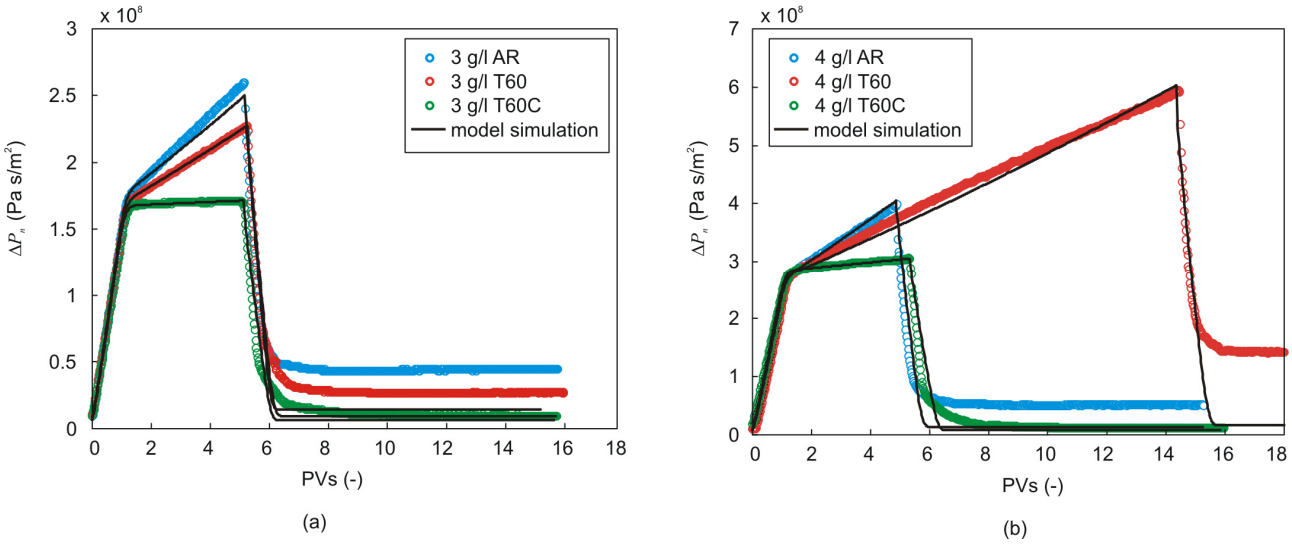

Figure 2: Normalized pressure drop $\Delta P_n = \Delta P/(Lq)$ over time for filtration tests of guar gum solutions at 3 g/l (a) and 4 g/l (b), prepared using different procedures. Pre-flushing data are not reported.

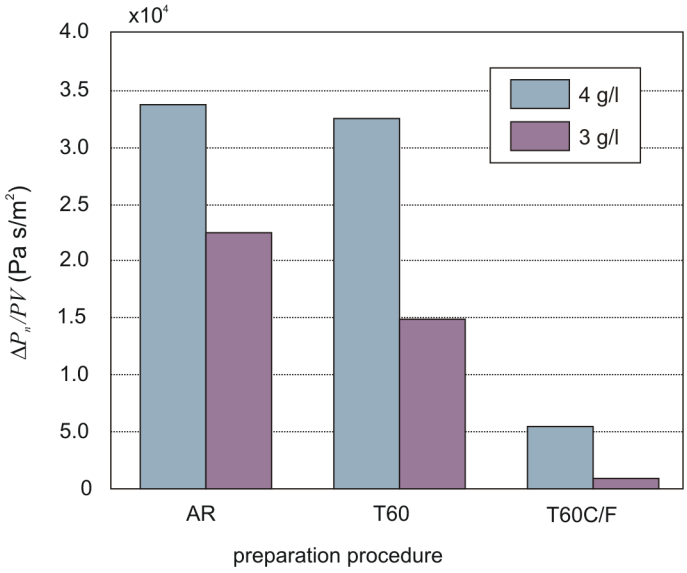

Figure 3: Porous medium clogging in filtration step tests, quantified as the slope of normalized pressure drop, $\Delta P_n/PV$.

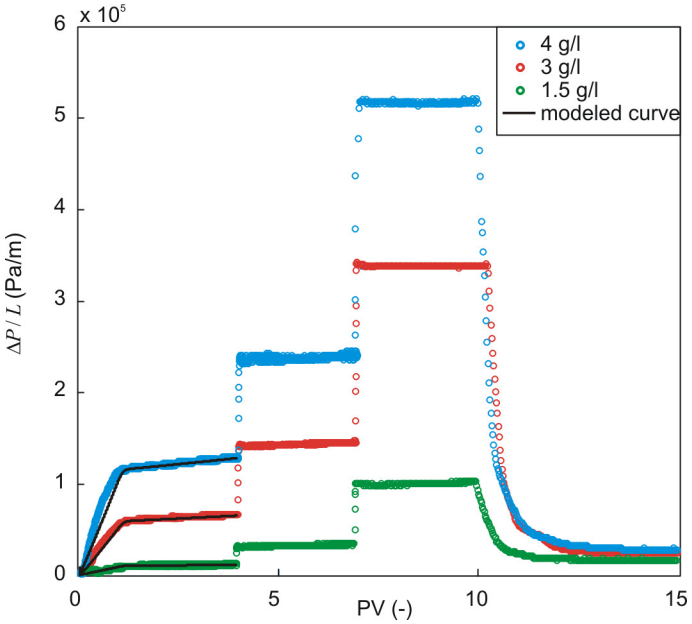

Figure 4: Pressure gradient for multi-step filtration tests: experimental data and modeled curves.

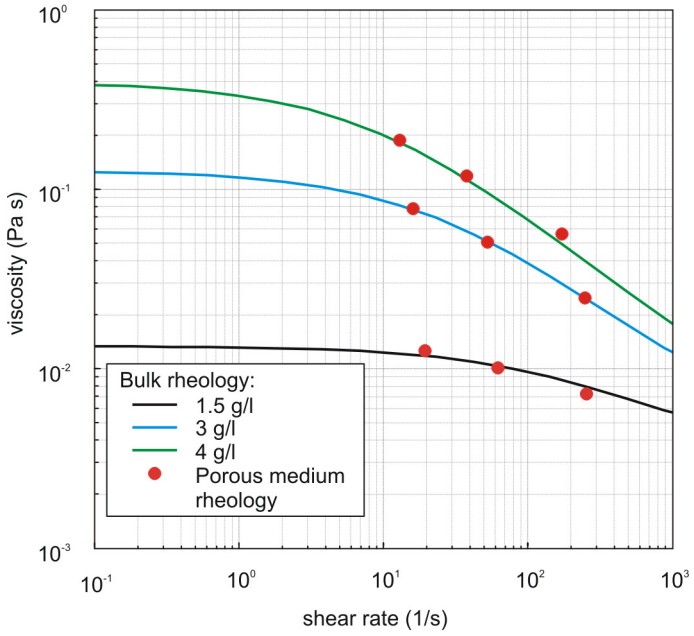

Figure 5: Bulk and porous medium rheology. Point values represent the apparent viscosity and shear rate calculated at the end of each injection step calculated from experimental pressure drop curves. Lines represent the bulk viscosity curves for the corresponding guar gum concentrations obtained from Cross curves in (Gastone et al., 2014).

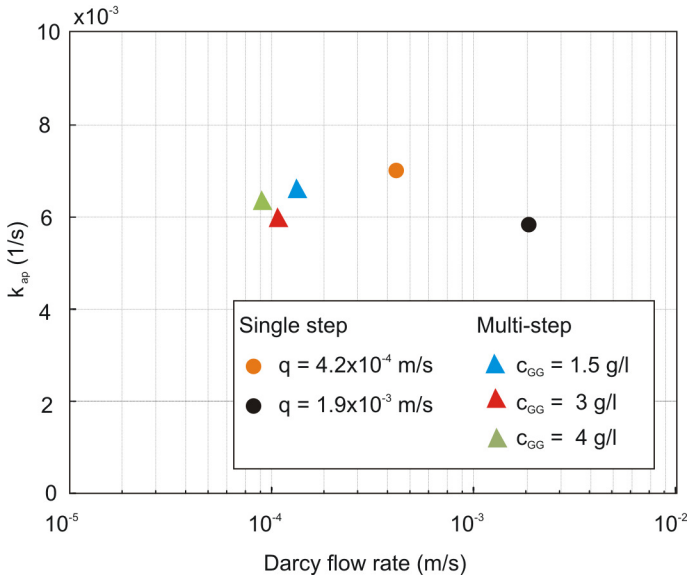

Figure 6: Filtration rate coefficients k_{ap} as a function of flow velocity for single-step tests (points), and the first step in multi-step tests (triangles).

Table captions

Table 1: Step filtration tests: test protocol (guar gum concentration, injected fluid, number of pore volumes for each step and Darcy velocity), experimental viscosity and shear rate in the porous medium.

					Experimental data	
c_{GG} (g/l)	Step	Fluid	PVs	q (m/s)	μ_m (Pa s)	$\dot{\gamma}_m$ (1/s)
1.5	Inj. step 1	GG	4	$1.39 \cdot 10^{-4}$	$1.26 \cdot 10^{-2}$	19.6
	Inj. step 2	GG	3	$4.22 \cdot 10^{-4}$	$1.01 \cdot 10^{-2}$	62.9
	Inj. step 3	GG	3	$1.71 \cdot 10^{-3}$	$7.21 \cdot 10^{-3}$	256.0
3	Inj. step 1	GG	4	$1.11 \cdot 10^{-4}$	$7.80 \cdot 10^{-2}$	16.1
	Inj. step 2	GG	3	$3.62 \cdot 10^{-4}$	$5.07 \cdot 10^{-2}$	53.0
	Inj. step 3	GG	3	$1.71 \cdot 10^{-3}$	$2.49 \cdot 10^{-2}$	250.8
4	Inj. step 1	GG	4	$9.06 \cdot 10^{-5}$	$1.87 \cdot 10^{-1}$	13.0
	Inj. step 2	GG	3	$2.65 \cdot 10^{-4}$	$1.19 \cdot 10^{-1}$	38.1
	Inj. step 3	GG	3	$1.22 \cdot 10^{-3}$	$5.61 \cdot 10^{-2}$	173.9

Table 2: Cross parameters of bulk viscosity curves from (Gastone et al., 2014) used in eq. (2) for the calculation of bulk viscosity in Figure 5.

μ_{GG} (g/l)	μ_0 (Pa s)	μ_∞ (Pa s)	λ (s)	χ (-)
1.5	0.014	$2.47 \cdot 10^{-3}$	$7.27 \cdot 10^{-3}$	0.57
3	0.167	$3.42 \cdot 10^{-3}$	$5.61 \cdot 10^{-2}$	0.68
4	0.487	$4.20 \cdot 10^{-3}$	$1.01 \cdot 10^{-1}$	0.74

Table 3: Clogging parameters obtained from inverse-fitting of single-step filtration tests.

Parameter	Test	Parameter value
a_p (m^2/m^3)	All tests	$2.01 \cdot 10^{7}$
k_a (s^{-1})	All tests	$5.86 \cdot 10^{-3}$
F (-)	TQ	0.12 (*)
	T60	$7.97 \cdot 10^{-2}$
	T60C	$1.14 \cdot 10^{-2}$
(*) Value not fitted (imposed a-priori).		

Table 4: Permeability coefficients estimated from single-step experimental results

Guar gum conc. c_{GG} (g/l)	Prep. method	Clean bed (initial) permeability k_0 (m^2)	Permeability at the end of GG injection $K_{end,inj}$ (m^2)	Permeability at the end of flushing $K_{end,flush}$ (m^2)	Darcy flow rate q (m/s)	Shear rate during injection $\dot{\gamma}_m$ (1/s)	Viscosity during injection μ_m (Pa s)
3	AR	$1.37 \cdot 10^{-10}$	$7.78 \cdot 10^{-11}$	$2.20 \cdot 10^{-11}$	1.93E-03	3.48E+02	2.02E-02
3	T60	$1.76 \cdot 10^{-10}$	$1.18 \cdot 10^{-10}$	$3.63 \cdot 10^{-11}$	1.98E-03	2.90E+02	2.67E-02
3	T60C	$1.49 \cdot 10^{-10}$	$1.46 \cdot 10^{-10}$	$1.02 \cdot 10^{-10}$	1.92E-03	2.53E+02	2.51E-02
4	AR	$1.68 \cdot 10^{-10}$	$7.54 \cdot 10^{-11}$	$2.04 \cdot 10^{-11}$	1.86E-03	3.40E+02	2.99E-02
4	T60	$1.45 \cdot 10^{-10}$	$6.01 \cdot 10^{-11}$	$6.27 \cdot 10^{-12}$	1.77E-03	3.63E+02	4.35E-02
4	T60C	$1.74 \cdot 10^{-10}$	$1.60 \cdot 10^{-10}$	$9.21 \cdot 10^{-11}$	1.91E-03	2.40E+02	4.84E-02